Available online at www.sciencedirect.com
SCIENCE DIRECT®
JOURNAL OF COMPUTATIONAL AND APPLIED MATHEMATICS
ELSEVIER
Journal of Computational and Applied Mathematics 168 (2004) 321–329
www.elsevier.com/locate/cam

Modelling of electromagnetic waves in periodic media with finite elements

André Nicolet[a,*], Sébastien Guenneau[b,1], Christophe Geuzaine[c], Frédéric Zolla[a]

[a] *Institut Fresnel, UMR 6133, Faculté de Saint-Jérôme case 162, Marseille Cedex 20 F13397, France*
[b] *Department of Mathematical Sciences, Peach Street, Liverpool L69 3BX, UK*
[c] *California Institute of Technology, Applied and Computational Mathematics, Pasadena CA 91125, USA*

Received 30 September 2002; received in revised form 8 July 2003

Abstract

Edge elements have been previously used to study electromagnetic waves conically propagating through a finite stack of arrays of fibres [(IEEE Trans. Magn. 38(2)(2002))]. This paper presents a new extension of this technique to the analysis of the propagation of such waves in a doubly periodic array of fibres. In the proposed approach, only the unit cell of the periodic material has to be meshed, thanks to Floquet–Bloch theory.

MSC: 65N25; 65N30; 78M10; 78A50

Keywords: Edge elements; Spectral problems; Bloch electromagnetic waves

1. Introduction

Photonic crystal research has renewed the interest for electromagnetic wave propagation in periodic structures. Though real structures are finite and one is often interested in the study of defects [3], the determination of modes in ideal periodic structures is of foremost importance. The Floquet–Bloch theory reduces the problem to the study of a single cell [5,6]. The purpose of this paper is to show how to combine this feature with finite element modelling in order to obtain numerical solutions for propagating modes in periodic structures.

* Corresponding author.
E-mail address: andre.nicolet@fresnel.fr (A. Nicolet).
[1] This work was undertaken while S. Guenneau was supported by the research grant GR/M93994.

0377-0427/$ - see front matter © 2003 Elsevier B.V. All rights reserved.
doi:10.1016/j.cam.2003.07.002

2. Spectral problem for conically propagating electromagnetic waves in doubly periodic structures

Let Y be the unit square cell $]0,1[\times]0,1[$. We consider a dielectric waveguide of constant cross section Ω in Y, invariant along the z-axis and whose permittivity profile ε is supposed to be a known function (e.g., a piecewise constant function). This unit cell is repeated periodically in the xy-plane (Fig. 1). We are looking for electromagnetic fields $(\mathscr{E},\mathscr{H})$ solutions of the following Maxwell equations:

$$\operatorname{curl}\mathscr{H} = \varepsilon\frac{\partial\mathscr{E}}{\partial t},$$
$$\operatorname{curl}\mathscr{E} = -\mu_0\frac{\partial\mathscr{H}}{\partial t}, \tag{2.1}$$

μ_0 being the permeability of vacuum. Furthermore, choosing a time dependence in $e^{-i\omega t}$, and taking into account the invariance of the guide along its z-axis, we define time-harmonic two-dimensional electric and magnetic fields $\mathbf{E}$ and $\mathbf{H}$ by

$$\mathscr{E}(x,y,z,t) = \Re e(\mathbf{E}(x,y)e^{-i(\omega t-\gamma z)}),$$
$$\mathscr{H}(x,y,z,t) = \Re e(\mathbf{H}(x,y)e^{-i(\omega t-\gamma z)}), \tag{2.2}$$

where ω is the angular frequency in the vacuum and where γ denotes the propagating constant of the guided mode. Note that $\mathbf{E}$ and $\mathbf{H}$ are complex valued fields depending on two variables (coordinates x and y) but still having three components (along the three axes). The structure being periodic in the xy-plane, our problem reduces to looking for Bloch waves solutions which are the solutions $\mathbf{U_k}$ that have the form (Bloch theorem [5])

$$\mathbf{U_k}(x,y) = e^{i\mathbf{k}\cdot\mathbf{r}}\mathbf{U}(x,y) = e^{i(k_x x+k_y y)}\mathbf{U}(x,y) \quad \text{for a.e. } (x,y) \text{ in } \mathbb{R}^2, \tag{2.3}$$

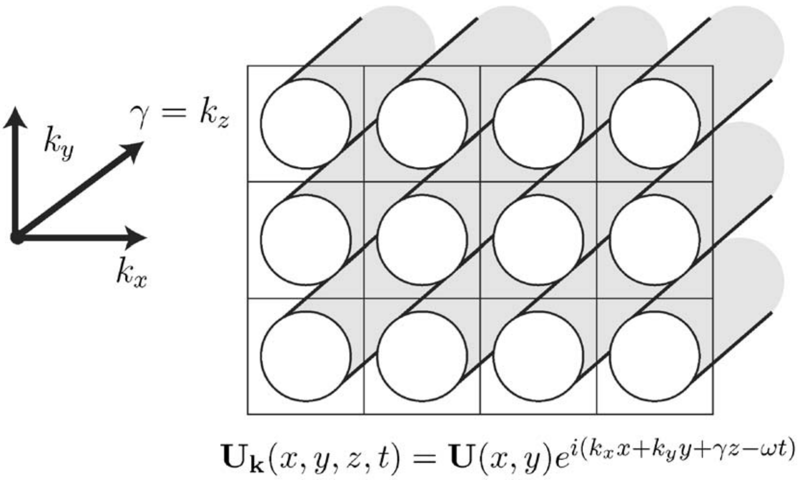

Fig. 1. A system with a translational invariance along the z-axis together with a two-dimensional periodicity in the xy-plane and the general form of propagating modes $\mathbf{U_k}(x,y,z,t)$.

where $\mathbf{k}=(k_x,k_y)\in\mathbb{R}^2$ is a parameter (the so-called Bloch vector or quasi-momentum in solid-state physics) and $\mathbf{U}(x,y)$ is a Y-periodic function, i.e., $\mathbf{U}(x+1,y)=\mathbf{U}(x,y+1)=\mathbf{U}(x,y)$. Such solutions are said to be $(\mathbf{k},Y)$-periodic in the sequel. To specify the class of solutions of our spectral problem, we introduce the Hilbert space $[L^2_\sharp(\mathbf{k},Y)]^3$ of $(\mathbf{k},Y)$-periodic square integrable functions on $Y\subset\mathbb{R}^2$ with values in $\mathbb{C}^3$. We say that the couple $(\mathbf{E_k},\mathbf{H_k})$ associated with the Bloch vector $\mathbf{k}$ is an *electromagnetic Bloch wave* if $(\mathbf{E_k},\mathbf{H_k})$ verifies (2.1) and is of the form specified by (2.2) and (2.3), with

$$\begin{aligned}
&(\gamma,\omega,\mathbf{k})\in\mathbb{R}_+\times\mathbb{R}_+\times\mathbb{R}^2,\\
&(\mathbf{E_k},\mathbf{H_k})\neq(\mathbf{0},\mathbf{0}),\\
&\mathbf{E_k},\mathbf{H_k}\in[L^2_\sharp(\mathbf{k},Y)]^3.
\end{aligned}\tag{2.4}$$

The Bloch wave can actually be thought of being born out of the interaction between the plane waves and the periodic medium. Looking for solutions that are Bloch functions in $[L^2_\sharp(\mathbf{k},Y)]^3$ ensures the well-posedness of our spectral problem, as a replacement of the Sommerfeld radiation condition (or other decaying conditions for the far field) which is usually imposed in the presence of compact obstacles in the medium. The following operators are defined:

$$\begin{aligned}
&\nabla_\gamma\varphi(x,y)=\nabla(\varphi(x,y)\mathrm{e}^{\mathrm{i}\gamma z})\mathrm{e}^{-\mathrm{i}\gamma z},\\
&\mathrm{curl}_\gamma\,\mathbf{U}(x,y)=\mathrm{curl}(\mathbf{U}(x,y)\mathrm{e}^{\mathrm{i}\gamma z})\mathrm{e}^{-\mathrm{i}\gamma z},\\
&\mathrm{div}_\gamma\,\mathbf{U}(x,y)=\mathrm{div}(\mathbf{U}(x,y)\mathrm{e}^{\mathrm{i}\gamma z})\mathrm{e}^{-\mathrm{i}\gamma z}.
\end{aligned}\tag{2.5}$$

The solutions $(\mathbf{E_k},\mathbf{H_k})$ of the spectral problem then satisfy

$$\begin{aligned}
&\mathrm{curl}_\gamma\,\mathbf{H_k}=-\mathrm{i}\omega\varepsilon_0\varepsilon_\mathrm{r}(x,y)\mathbf{E_k},\\
&\mathrm{curl}_\gamma\,\mathbf{E}_\mathrm{k}=\mathrm{i}\omega\mu_0\mathbf{H}_\mathrm{k},
\end{aligned}\tag{2.6}$$

where ε_r denotes the relative permittivity (bounded and coercive function on Y). Note that $\mathrm{curl}_\gamma\nabla_\gamma\varphi=0$ for smooth scalar fields φ and that $\mathrm{div}_\gamma\,\mathrm{curl}_\gamma\,\mathbf{U}=0$ for smooth vector fields $\mathbf{U}$.

3. Finite element modelling of the eigenvalue problem

3.1. The magnetic formulation for a dielectric inclusion

Eliminating the electric field from (2.6), one finds

$$\mathrm{curl}_\gamma\frac{1}{\varepsilon_\mathrm{r}}\mathrm{curl}_\gamma\,\mathbf{H_k}=k_0^2\mathbf{H_k},\tag{3.7}$$

where $k_0^2=\varepsilon_0\mu_0\omega^2=\omega^2/c^2$. The weak form of this equation together with the constraint $\mathrm{div}_\gamma\,\mathbf{H_k}=0$ corresponds to the problem of annulling the following residues ($\bar{\mathbf{H}}$ denotes the complex conjugate of $\mathbf{H}$):

$$\mathscr{R}(\gamma;\mathbf{H_k},\mathbf{H'_k}) = \int_Y \frac{1}{\varepsilon_r}\,\mathrm{curl}_\gamma\,\mathbf{H_k}\cdot\overline{\mathrm{curl}_\gamma\,\mathbf{H'}_\mathbf{k}}\,\mathrm{d}x\,\mathrm{d}y$$

$$+s\int_Y \mathrm{div}_\gamma\,\mathbf{H_k}\,\overline{\mathrm{div}_\gamma\,\mathbf{H'_k}}\,\mathrm{d}x\,\mathrm{d}y - k_0^2\int_Y \mathbf{H_k}\cdot\overline{\mathbf{H'}_\mathbf{k}}\,\mathrm{d}x\,\mathrm{d}y. \tag{3.8}$$

Here $\mathbf{H'_k}$ is the weight vector field chosen in the same space as $\mathbf{H_k}$, the unknown magnetic field. This problem of minimization admits a unique solution thanks to the penalty term $s\int_Y \mathrm{div}_\gamma\,\mathbf{H_k}\,\overline{\mathrm{div}_\gamma\,\mathbf{H'_k}}\,\mathrm{d}x\,\mathrm{d}y$ (where s is an arbitrary multiplier) which acts as a constraint forcing the nullity of $\mathrm{div}_\gamma\,\mathbf{H_k}$ in Y. The numerical formulation is given by the following residue [4,7]

$$\mathscr{R}(\gamma;\mathbf{H_k},\mathbf{H'_k}) = \int_Y \varepsilon_r^{-1}(\mathrm{curl}_t\,\mathbf{H}_{t,\mathbf{k}}\cdot\mathrm{curl}_t\,\overline{\mathbf{H}'_{t,\mathbf{k}}} + \nabla_t H_{l,\mathbf{k}}\cdot\nabla_t\bar{H}'_{l,\mathbf{k}}$$

$$-\mathrm{i}\gamma(\mathbf{H}_{t,\mathbf{k}}\cdot\nabla_t\overline{H'}_{l,\mathbf{k}} - \nabla_t H_{l,\mathbf{k}}\cdot\overline{\mathbf{H}'_{t,\mathbf{k}}}) + \gamma^2\mathbf{H}_{t,\mathbf{k}}\cdot\overline{\mathbf{H}'_{t,\mathbf{k}}})\,\mathrm{d}x\,\mathrm{d}y$$

$$-k_0^2\int_Y(\mathbf{H}_{t,\mathbf{k}}\cdot\overline{\mathbf{H}'_{t,\mathbf{k}}} + H_{l,\mathbf{k}}\overline{H'_{l,\mathbf{k}}})\,\mathrm{d}x\,\mathrm{d}y, \tag{3.9}$$

where the unknown field now belongs to a discrete Hilbert space (i.e., with a finite dimension equal to the number of numerical parameters to be determined). This formulation involves both a transverse field $\mathbf{H}_{t,\mathbf{k}}$ in the section of the guide and a longitudinal field $H_{l,\mathbf{k}}$ along its axis such that

$$\mathbf{H_k} = \mathbf{H}_{t,\mathbf{k}} + H_{l,\mathbf{k}}\mathbf{e_z} \tag{3.10}$$

and curl_γ has been developed in its transverse and longitudinal components

$$\mathrm{curl}_\gamma\,\mathbf{H_k} = \mathrm{curl}_t\,\mathbf{H}_{t,\mathbf{k}}\mathbf{e_z} + (\nabla_t H_{l,\mathbf{k}} - \mathrm{i}\gamma\mathbf{H}_{t,\mathbf{k}})\times\mathbf{e_z}. \tag{3.11}$$

The section of the guide is meshed with triangles and Whitney finite elements [1] are used, i.e., edge elements for the transverse field and node elements for the longitudinal field:

$$\mathbf{H_k} = \begin{cases} \mathbf{H}_{t,\mathbf{k}} = \sum_{\text{edges } i} \alpha_i \mathbf{w^e_i}(x,y), \\ H_{l,\mathbf{k}} = \sum_{\text{nodes } j} \beta_j w^n_j(x,y), \end{cases} \tag{3.12}$$

where α_i denotes the line integral of the transverse component $\mathbf{H}_{t,\mathbf{k}}$ on the edges, and β_j denotes the line integral of the longitudinal component $H_{l,\mathbf{k}}$ along one unit of length of the axis of the guide (what is equivalent to a nodal value). Besides, $w^n_j(x,y)=\lambda_j(x,y)$ and $\mathbf{w^e_i}=\lambda_k(x,y)\nabla\lambda_l(x,y)-\lambda_l(x,y)\nabla\lambda_k(x,y)$ (where λ_i is the barycentric coordinate of node i and the edge $\mathbf{i}$ has nodes (k and l as extremities) are, respectively, the basis functions of Whitney 1-forms (edge element discrete space W^1) and Whitney 0-forms (nodal element discrete space W^0). The use of the Whitney elements solves the spurious mode problem in a way similar to the one of the cavities [1]. To see that, it has to be noticed that the penalty term involving the divergence is not introduced in the discrete formulation because the use of Whitney elements guarantees the nullity of the divergence in a weak sense. One of the main properties of the edge element space (Whitney 1-forms) is that it includes exactly the gradients of the node element approximation functions (gradients of Whitney 0-forms). It is therefore possible to choose

$$\mathbf{H}'_{\mathbf{k}} = \nabla_\gamma \varphi. \tag{3.13}$$

Taking $s = 0$ (i.e., neglecting the penalty term for the divergence) and introducing (3.13) in (3.8), one obtains, since $\mathrm{curl}_\gamma \nabla_\gamma \varphi = 0$:

$$\int_Y \mathbf{H}_{\mathbf{k}} \cdot \overline{\nabla_\gamma \varphi}\, \mathrm{d}x\, \mathrm{d}y = 0, \quad \forall \varphi \in W^0 \tag{3.14}$$

for all $\omega \neq 0$. Eq. (3.14) is indeed a weak form of $\mathrm{div}_\gamma\, \mathbf{H}_{\mathbf{k}} = 0$. As the eigenvalue problem involves, on the one side, k_0^2 only and, on the other side, both γ and γ^2, a more classical (though generalized) eigenvalue problem is obtained by fixing $\gamma \in \mathbb{R}_+$ for a given Bloch vector $\mathbf{k}$ and looking for $(k_0^2, \mathbf{H}_{\mathbf{k}})$ satisfying the discrete spectral problem.

3.2. The electric formulation for a metallic inclusion

If we consider a (perfectly conducting) metallic inclusion Ω_m in the basic cell Y, the presence of metallic walls introduces unknown surface currents equal to the tangential component of the magnetic field. The magnetic formulation is not well suited to take into account such metallic boundary conditions and therefore we choose now an electric field formulation (dual to the magnetic one) to get simple boundary conditions because the tangential component of the electric field is null. The magnetic field is first eliminated from (2.6) to give

$$\mathrm{curl}_\gamma\, \mathrm{curl}_\gamma\, \mathbf{E}_{\mathbf{k}} = \varepsilon \mu_0 \omega^2 \mathbf{E}_{\mathbf{k}}. \tag{3.15}$$

The weak form of this equation together with the constraint $\mathrm{div}_\gamma \varepsilon \mathbf{E}_{\mathbf{k}} = 0$ corresponds to minimizing the following functional in the weighted Hilbert space $[H_\sharp(Y \setminus \Omega_m, \mathrm{d}\mathscr{L})]^3$, where $\mathrm{d}\mathscr{L}$ is the Lebesgue measure $\varepsilon_{\mathrm{r}}^{-1}\, \mathrm{d}x\, \mathrm{d}y$:

$$\begin{aligned}\mathscr{R}(\gamma; \mathbf{E}_{\mathbf{k}}, \mathbf{E}'_{\mathbf{k}}) = {} & \int_{Y \setminus \Omega_m} \mathrm{curl}_\gamma\, \mathbf{E}_{\mathbf{k}} \cdot \overline{\mathrm{curl}_\gamma\, \mathbf{E}'_{\mathbf{k}}}\, \mathrm{d}\mathscr{L} \\ & + s \int_{Y \setminus \Omega_m} \mathrm{div}_\gamma\, \mathbf{E}_{\mathbf{k}} \overline{\mathrm{div}_\gamma\, \mathbf{E}'_{\mathbf{k}}}\, \mathrm{d}\mathscr{L} - \frac{\omega^2}{c^2} \int_{Y \setminus \Omega_m} \mathbf{E}_{\mathbf{k}} \cdot \overline{\mathbf{E}'_{\mathbf{k}}}\, \mathrm{d}\mathscr{L}.\end{aligned} \tag{3.16}$$

We introduce finite elements in a way similar to the magnetic formulation. Whitney finite elements are used for the electric field, i.e., edge elements for the transverse field and nodal elements for the longitudinal field:

$$\mathbf{E}_{\mathbf{k}} = \begin{cases} \mathbf{E}_{t,\mathbf{k}} = \displaystyle\sum_{\text{edges } i} \alpha_i \mathbf{w}_{\mathbf{i}}^{\mathbf{e}}(x, y), \\ E_{l,\mathbf{k}} = \displaystyle\sum_{\text{nodes } j} \beta_j w_j^n(x, y), \end{cases} \tag{3.17}$$

where α_j denotes the line integral of the transverse component $\mathbf{E}_{t,\mathbf{k}}$ on the edges, and β_j denotes the line integral of the longitudinal component $E_{l,\mathbf{k}}$ along one unit of length of the axis of the guide. The operator curl_γ is again developed in its transverse and longitudinal components and the final expression of the functional to minimize can be written as

$$\mathscr{R}(\gamma;\mathbf{E}_\mathbf{k},\mathbf{E}'_\mathbf{k}) = \int_{Y\setminus\Omega_m} (\mathrm{curl}_t\,\mathbf{E}_{t,\mathbf{k}}\cdot\mathrm{curl}_t\,\overline{\mathbf{E}'_{t,\mathbf{k}}} + \nabla_t E_{l,\mathbf{k}}\cdot\nabla_t\bar{E}'_{l,\mathbf{k}}$$
$$-\mathrm{i}\gamma(\mathbf{E}_{t,\mathbf{k}}\cdot\nabla_t\overline{E'_{l,\mathbf{k}}} - \nabla_t E_{l,\mathbf{k}}\cdot\overline{\mathbf{E}'_{t,\mathbf{k}}}) + \gamma^2\mathbf{E}_{t,\mathbf{k}}\cdot\overline{\mathbf{E}'_{t,\mathbf{k}}})\,\mathrm{d}\mathscr{L}$$
$$-\mu_0\omega^2\int_{Y\setminus\Omega_m}(\mathbf{E}_{t,\mathbf{k}}\cdot\overline{\mathbf{E}'_{t,\mathbf{k}}} + E_{l,\mathbf{k}}\overline{E'_{l,\mathbf{k}}})\,\mathrm{d}\mathscr{L}. \tag{3.18}$$

As in the case of the magnetic field formulation, it is interesting to notice that the penalty term involving the divergence is not introduced in the discrete formulation because the use of Whitney elements guarantees the nullity of the divergence in a weak sense i.e., $\int_{Y\setminus\Omega_m}\mathbf{E}_\mathbf{k}\cdot\overline{\nabla_\gamma\varphi}\,\mathrm{d}\mathscr{L}=0$, for all $\varphi\in W^0$ and for all $\omega\neq 0$.

3.3. The Bloch conditions

In order to find Bloch modes with the finite element method, some changes have to be performed with respect to classical boundary value problems that will be named *Bloch conditions* [6]. To avoid tedious notations, let us consider the case of a scalar field $U_\mathbf{k}(x,y)$ (time and z dependence are irrelevant here and there is no particular problem to extend this method to vector quantities and edge elements) on the square cell Y with Bloch conditions relating the left and the right side (Fig. 2). The set of nodes is separated in three subsets: the nodes on the left side, i.e., with $x=0$, corresponding to the column array of unknowns $\mathbf{u_l}$, the nodes on the right side, i.e., with $x=1$,

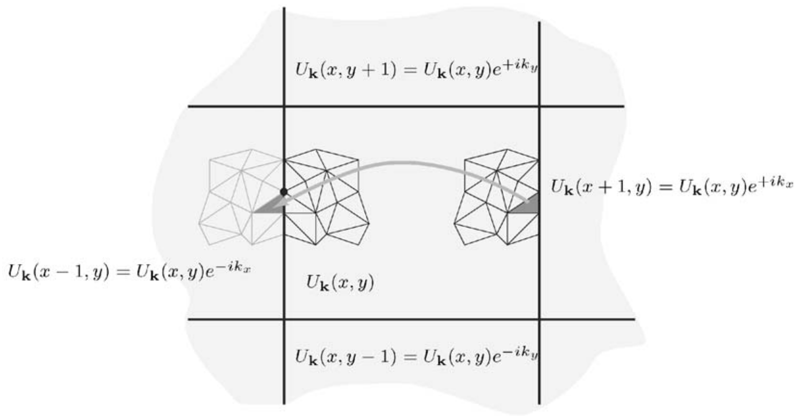

Fig. 2. Bloch theorem and virtual periodic meshing.

corresponding to the column array of unknowns $\mathbf{u_r}$, and the internal nodes, i.e., with $x \in]0,1[$, corresponding to the column array of unknowns $\mathbf{u}$. One has the following structure for the matrix problem (corresponding in fact to natural boundary conditions, i.e., Neumann homogeneous boundary conditions):

$$\mathbf{A}\begin{pmatrix}\mathbf{u}\\ \mathbf{u_l}\\ \mathbf{u_r}\end{pmatrix} = \mathbf{b}, \tag{3.19}$$

where $\mathbf{A}$ is the (square Hermitian) matrix of the system and $\mathbf{b}$ the right-hand side. The solution to be approximated by the numerical method is a Bloch function $U_{\mathbf{k}}(x,y) = U(x,y)\mathrm{e}^{\mathrm{i}(k_x x + k_y y)}$ with U being Y-periodic and in particular $U(x+1,y) = U(x,y)$. Therefore, the relation between the left and the right side is:

$$U_{\mathbf{k}}(1,y) = U(1,y)\mathrm{e}^{\mathrm{i}(k_x + k_y y)} = U_{\mathbf{k}}(0,y)\mathrm{e}^{\mathrm{i}k_x} \Rightarrow \mathbf{u}_{\mathrm{r}} = \mathbf{u_l}\mathrm{e}^{\mathrm{i}k_x}.$$

The set of unknowns can thus be expressed in function of the reduced set $\mathbf{u}$ and $\mathbf{u_l}$ thanks to

$$\begin{pmatrix}\mathbf{u}\\ \mathbf{u_l}\\ \mathbf{u_r}\end{pmatrix} = \mathbf{P}\begin{pmatrix}\mathbf{u}\\ \mathbf{u_l}\end{pmatrix} \quad \text{with } \mathbf{P} = \begin{pmatrix}\mathbf{1} & \mathbf{0}\\ \mathbf{0} & \mathbf{1}\\ \mathbf{0} & \mathbf{1}\mathrm{e}^{\mathrm{i}k_x}\end{pmatrix}, \tag{3.20}$$

where $\mathbf{1}$ and $\mathbf{0}$ are identity and null matrices, respectively, with suitable dimensions. The finite element equations related to the eliminated nodes have now to be taken into account. Thanks to the periodicity of the structure, the elements on the left of the right side correspond to elements on the left of the left side (Fig. 2). Therefore their contributions (i.e., equations corresponding to $\mathbf{u_r}$) must be added to the equations corresponding to $\mathbf{u_l}$ with the right phase factor, i.e., $\mathrm{e}^{-\mathrm{i}k_x}$, which amounts to multiply the system matrix by $\mathbf{P}^*$ (the Hermitian of $\mathbf{P}$). Finally, the linear system to be solved is

$$\mathbf{P}^*\mathbf{A}\mathbf{P}\begin{pmatrix}\mathbf{u}\\ \mathbf{u_l}\end{pmatrix} = \mathbf{P}^*\mathbf{b}, \tag{3.21}$$

where it is worth noting that the system matrix is still Hermitian, which is important for numerical computation. Now a generalized eigenvalue problem (with natural boundary conditions) $\mathbf{Au} = \lambda\mathbf{Bu}$ is transformed to a Bloch mode problem according to $\mathbf{P}^*\mathbf{APu}' = \lambda\mathbf{P}^*\mathbf{BPu}'$. Such problems involving large sparse Hermitian matrices can be solved using a Lanczos algorithm, which permits to compute their largest eigenvalues [7]. Since we are in fact interested in the smallest eigenvalues, the inverse of $\mathbf{A}$ must be used in the iterations. Of course, the inverse is never computed explicitly but the matrix-vector products are replaced by system solutions thanks to a GMRES method [8]. It is therefore obvious that the numerical efficiency of the process relies strongly on Krylov subspace techniques and the Arnoldi iteration algorithm [8]. The practical implementation of the model has been performed thanks to the *GetDP* software [2].

4. Numerical results

In order to avoid huge constants in numerical computations, normalized units have been chosen where $c = \sqrt{\varepsilon_0 \mu_0} = 1$ and the unit of length is the side length of the cell. For instance, if one considers a real cell of size 1 μm, k_x, k_y and γ must be multiplied by 10^6 to get their values and ω must be multiplied by about $3 \cdot 10^{14}$. As an illustration, the case of a circular metallic inclusion (radius = 0.4 m) in a unit square cell has been considered. Fig. 3 shows a particular mode. Using a 660 triangle mesh, the determination of the first half dozen of modes takes only a few seconds with a 1 GHz processor. Though the solution is computed only on one cell, it has been reconstructed on a 2×3 cell set by multiplying by the phase factor ($e^{i(nk_x+mk_y)}$ for cell (n,m)). It has to be observed that this non-periodic solution is continuous between cells, which is a clue showing that we are in presence of a Bloch mode. (In this section, 'continuous' has not to be taken in its mathematical acception but in the more intuitive sense that the graphical representation of the vector field is likely to correspond to a continuous one.) Fig. 4 shows a band diagram for a given propagation

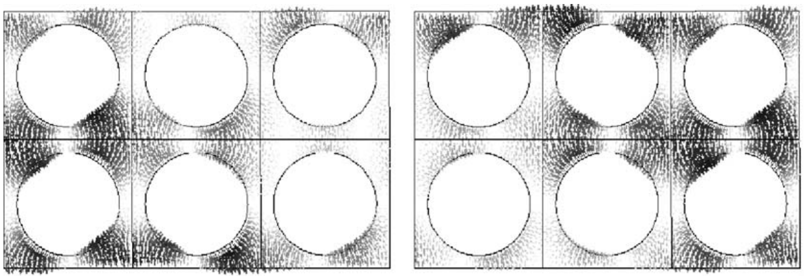

Fig. 3. Bloch mode ($\gamma = 7\ \mathrm{m}^{-1}, k_x = 1.2\ \pi\ \mathrm{m}^{-1}, k_y = 0.2\ \pi\ \mathrm{m}^{-1}, \omega = 8 \cdot 14\ \mathrm{s}^{-1}$) shown on 2×3 cells (real part (on the left) and imaginary part (on the right) of the transverse electric field).

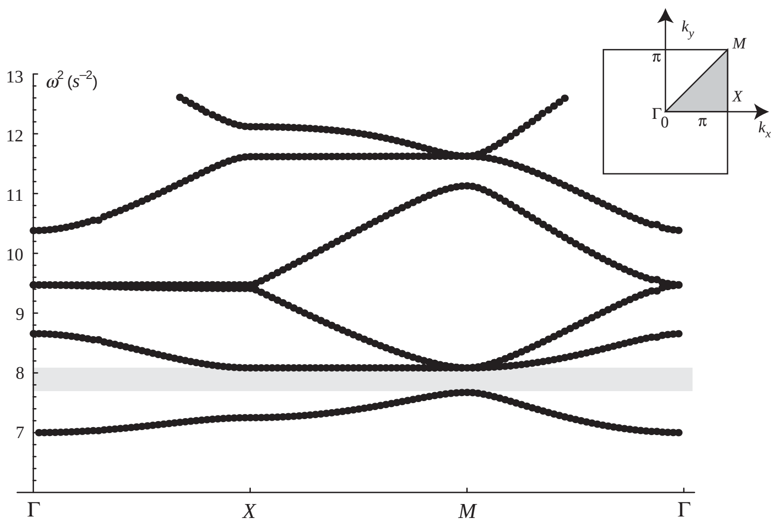

Fig. 4. Band diagram for $\gamma = 7\ \mathrm{m}^{-1}$ on the boundary of the irreducible part of the Brillouin zone of the reciprocal square lattice.

constant ($\gamma = 7\ \mathrm{m}^{-1}$). The Bloch vector varies conventionally on the boundary of the irreducible part of the first Brillouin zone (the momentum space dual of the Y-cell). A gap appears just above the bottom curve indicating that interesting guiding properties for the given propagation constant may be expected in this structure possibly modified by the introduction of defects.

5. Conclusion

In this paper the application of the finite element method to photonic crystal waveguides via the implementation of Floquet–Bloch conditions has been presented. Although a very simple geometry has been considered, one of the main advantages of this approach with respect to more usual methods in the field is its extreme flexibility with respect to the geometry and the material characteristics of the problem. Reversing the optical index contrast, introducing one or several defects or disturbing the shape or the pattern of the elements of the photonic crystal is not a problem. Future work will concern the exploration of the effect of a slight perturbation of the periodicity of the lattice (e.g., by considering a “random” or “quasi-periodic” set of fibres in a macrocell) on the band diagrams.

References

[1] A. Bossavit, Solving Maxwell equations in a closed cavity, and the question of spurious modes, IEEE Trans. Magn. 26 (2) (1990), pp. 702–705.
[2] P. Dular, C. Geuzaine, F. Henrotte, W. Legros, A general environment for the treatment of discrete problems and its application to the finite element method, IEEE Trans. Magn. 34 (5) (1998) 3395–3398, See also the Internet address http://www.geuz.org/getdp/.
[3] S. Guenneau, A. Nicolet, F. Zolla, S. Lasquellec, Modeling of photonic crystal optical fibers with finite elements, IEEE Trans. Magn. 38 (2) (2002).
[4] S. Guenneau, A. Nicolet, F. Zolla, C. Geuzaine, B. Meys, A finite element formulation for spectral problems in optical fibers, COMPEL 20 (1) (2001) 120–131.
[5] C. Kittel, Introduction to Solid State Physics, Wiley, New York, 1996.
[6] Ph. Langlet, A.-C. Hladky-Hennion, J.-N. Decarpigny, Analysis of the propagation of plane acoustic waves in passive periodic materials using the finite element method, J. Acoust. Soc. Amer. 98 (5, Part 1) (1995) 2792–2800.
[7] B. Meys, Ph.D. Thesis, Université de Liège, 1999.
[8] L.N. Trefethen, D. Bau III, Numerical Linear Algebra, SIAM, Philadelphia, 1997.